Soft Matter

View Online
Dynamic Article Links

Cite this: DOI: 10.1039/c1sm05046j

www.rsc.org/softmatter

PAPER

Photocontrol of end-grafted lambda-phage DNA

Yuting Liang Sun,[a] Naresh Kumar Mani,[bcd] Damien Baigl,[bcd] Thomas Gisler,[e] André Pierre Schröder[a] and Carlos Manuel Marques*[a]

Received 12th January 2011, Accepted 14th March 2011
DOI: 10.1039/c1sm05046j

We study the response to light stimulation of end-grafted λ-phage DNAs in a solution of AzoTAB, a photosensitive compacting agent for the DNA chains. The biotinylated double-stranded DNA molecules are end-attached to a streptavidinated substrate and incubated in a 120 mM tris-borate-EDTA buffer in the presence of the cationic surfactant AzoTAB. We find that the conformations and the dynamics of the tethered DNAs can be tuned by the AzoTAB concentration and strongly depend on illumination conditions. Under visible light or in the dark AzoTAB is in a *trans* configuration and it induces DNA adsorption onto the substrate for [AzoTAB] ≥ 0.3 mM. In contrast, under UV illumination, AzoTAB is in a *cis* configuration and it induces DNA adsorption for [AzoTAB] ≥ 0.4 mM. In the AzoTAB concentration range 0.3–0.4 mM, one can thus reversibly switch between the adsorbed and the non-adsorbed states of the end-grafted chains by exposing the sample respectively to visible light (>400 nm) and to UV illumination (365 nm). These light-induced adsorption transitions occur for AzoTAB concentrations approximately half of those required to control the DNA conformation in bulk solution, which highlights the predominance of chain-surface interactions over monomer-monomer intra-chain interactions for DNA molecules in the close vicinity of a solid substrate.

1 Introduction

Achieving light control of end-grafted chains has been the cornerstone in the design of photoresponsive systems such as microfluidic devices,[1] chemical gates and chemical valves,[2] nano-platforms for *in vivo* drug-delivery[3] and many others where properties of surfaces are tuned by changes in the conformations of the attached polymer layers.[4] Although extensive efforts have been made to correlate polymer architecture or conditions in the polymer environment to the final effects induced by the light, there is a lack of experimental geometries where the evolution of end-attached chain conformations can be directly monitored upon irradiation. Developments of such model experiments would not only pave the way for connecting individual chain conformations to global surface properties, but would also bring new insight into the longstanding problem of the collapsing and adsorption transitions in end-grafted polymers,[5,6] as depicted in Fig. 1.

The conformations of single DNAs in bulk solution can be photocontrolled by adding to the DNA solution a cationic surfactant that contains a photosensitive moiety in its hydrophobic part.[7,8] Several of these photosensitive surfactants have

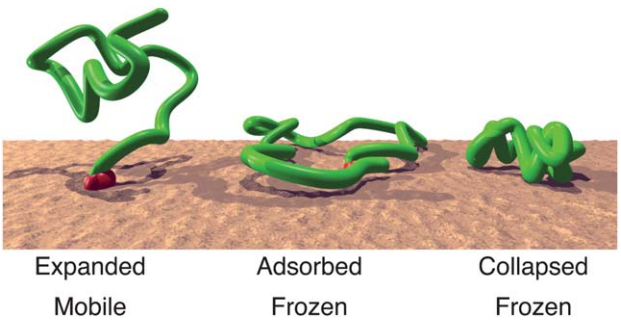

Fig. 1 A sketch of the three different conformations of end-grafted λ-phage DNA molecules observed in this study. In the left, at low AzoTAB concentrations, without enough attractive interactions between the chain and the substrate, the chain is fully mobile under thermal forces, with the restrictions imposed to the motion by the end-attached point and by the impenetrable wall. In the middle, at intermediate concentrations of AzoTAB, the presence of attractions between the chain and the substrate leads to adsorbed conformations that appear frozen at the optical length scales. In the right, a collapsed chain conformation at higher AzoTAB concentrations, when intra-chain attractions play a significant role.

[a]*Institut Charles Sadron, Université de Strasbourg, CNRS UP 22, 23 rue du Loess, Strasbourg Cedex, 67083, France. E-mail: marques@unistra.fr; Fax: +33 388 414 099; Tel: +33 388 414 045*
[b]*Department of Chemistry, Ecole Normale Supérieure, 75005 Paris, France*
[c]*Université Pierre et Marie Curie Paris 6, 75005 Paris, France*
[d]*UMR 8640, CNRS, France*
[e]*Fachbereich Physik, Universität Konstanz, Fach M621, 78457 Konstanz, Germany*

been successfully proposed, such as gemini surfactants[9] and linear surfactants with various hydrophobicities,[10] but the most widely used molecule is AzoTAB, a trimethylammonium bromide surfactant containing an azobenzene group in its short hydrophobic tail.[7–12] When irradiated at 365 nm, AzoTAB undergoes a *trans* to *cis* isomerization accompanied by a change of polarity[12] (CMC = 12.6 mM and 14.6 mM for *trans* and *cis* isomers, respectively[10]). It has been shown that this polarity change is accompanied by a change of its affinity for DNA.[7–10] *Trans*-AzoTAB has a stronger affinity for DNA and induces DNA compaction at a lower concentration than its more polar form *cis*-AzoTAB. As a consequence there exists an AzoTAB concentration range for which DNA is compacted under visible light conditions (>400 nm) but unfolded under UV illumination (365 nm). These light-induced conformational changes have been studied in bulk[7–10] and in cell-mimicking micro-environments[8] and were applied to control gene expression systems using light.[11]

Unprecedented scrutiny of the equilibrium and out-of-equilibrium conformations of single DNAs near an impenetrable wall has been achieved by advances in the preparation of well defined surfaces with end-grafted DNA chains as well as by developments in quantitative fluorescence microscopy of single-DNA molecules.[13,14] In this paper we combine such techniques with the photocontrol power of AzoTAB to study for the first time the changes in conformations and dynamics of individual end-grafted DNA molecules in response to different light stimuli.

2 Results and discussion

The present study relies on our ability to determine the dynamic conformation state of end-grafted DNA chains in the presence of various concentrations of AzoTAB. In particular, we need to evaluate the progressive loss of mobility of the DNA chains as the AzoTAB concentration increases leading to a significant number of intra-chain and chain-substrate attractive interactions. In previous work[8,9] of free standing DNA chains in solutions, where only intra-chain bonds take place, the effect of attractive attractions induced by AzoTAB has been evaluated by studying the average optical size of DNA chains. In our case of end-grafted DNA chains, where chain-surface attractions play a significant role, chain size alone cannot discriminate between mobile and frozen states of the DNAs. We introduce here a new method—see Section 3.5—that enables assessing by simple image analysis the immobilization degree of an end-grafted DNA chain above optical image resolution, in our case for length scales above 0.3 μm. The results of this method are illustrated in Fig. 2 for DNA chains in 120 mM tris-borate-EDTA buffer (TBE) without—Fig. 2A(a–f)—and with—Fig. 2B(a–f)—AzoTAB. When the chains are mobile, our method leads to a composite image in green and red—Fig. 2A(f)—where the green component indicates the average monomer concentration and the red channel shows our measure of mobility. Composite images only in green—Fig. 2B(f)—are observed for frozen DNAs, *i.e.* for chains that do not display any conformation changes at the optical length scales, within the few minutes available for experiments.

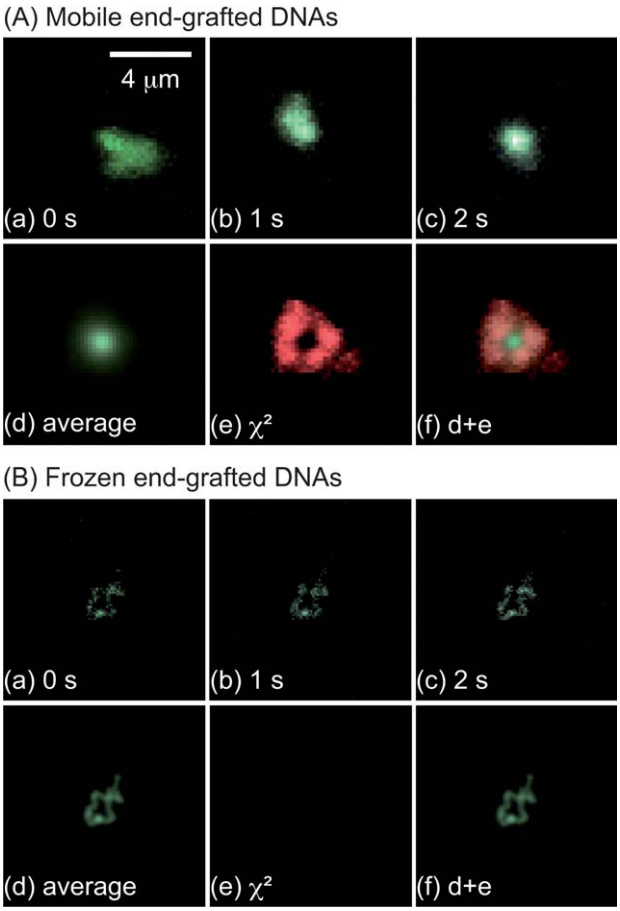

Fig. 2 Assessment of DNA mobility by image analysis. (A) End-grafted DNA in 120 mM tris-borate-EDTA buffer (TBE). (a)–(c) Typical fluorescence microscopy snapshots: original fluorescence intensity was recorded with 16-bit resolution at 8 frames per second, and then displayed in the green channel of a RGB image. (d) Average image of 37 snapshots, where the fluctuations of conformation lead to an isotropic distribution of fluorescence intensity centered on the end-grafted position. (e) χ^2-image—see text for a full description—displaying in the red channel the relative value of light intensity fluctuations for the 37 snapshots. The center of the pattern is dark, and corresponds to a region with high light intensity and small relative fluctuations. Far from the center one recovers background fluctuations (noise of the camera) which have been subtracted. The larger values of χ^2 are thus exhibited at intermediate distances from the center where DNA motion results in high relative light fluctuations. (f) Composite RGB image that combines the average (d) and χ^2 (e) images. According to the image analysis method developed here, single-DNA mobility and fluctuations of conformation result in the presence of a red halo in the composite images. (B) End-grafted DNA molecule in the same TBE buffer with added 0.6 mM of *trans*-AzoTAB. (a)–(f) Fluorescence snapshots, acquired, analyzed and displayed as in (A). Non isotropic distribution of light intensity in (d) and absence of red halo in (f) show that the DNA molecule is in a frozen conformation.

2.1 End-grafted DNAs in a *trans*-AzoTAB solution

We studied the end-grafted DNA conformations in a buffer (TBE) solution with increasing concentrations of *trans*-AzoTAB, in the range 0–2 mM. Fig. 3A shows typical composite images of DNA using the image analysis method described in Fig. 2. The images show that the chains exhibit significant mobility for AzoTAB concentrations below 0.3 mM. For concentrations

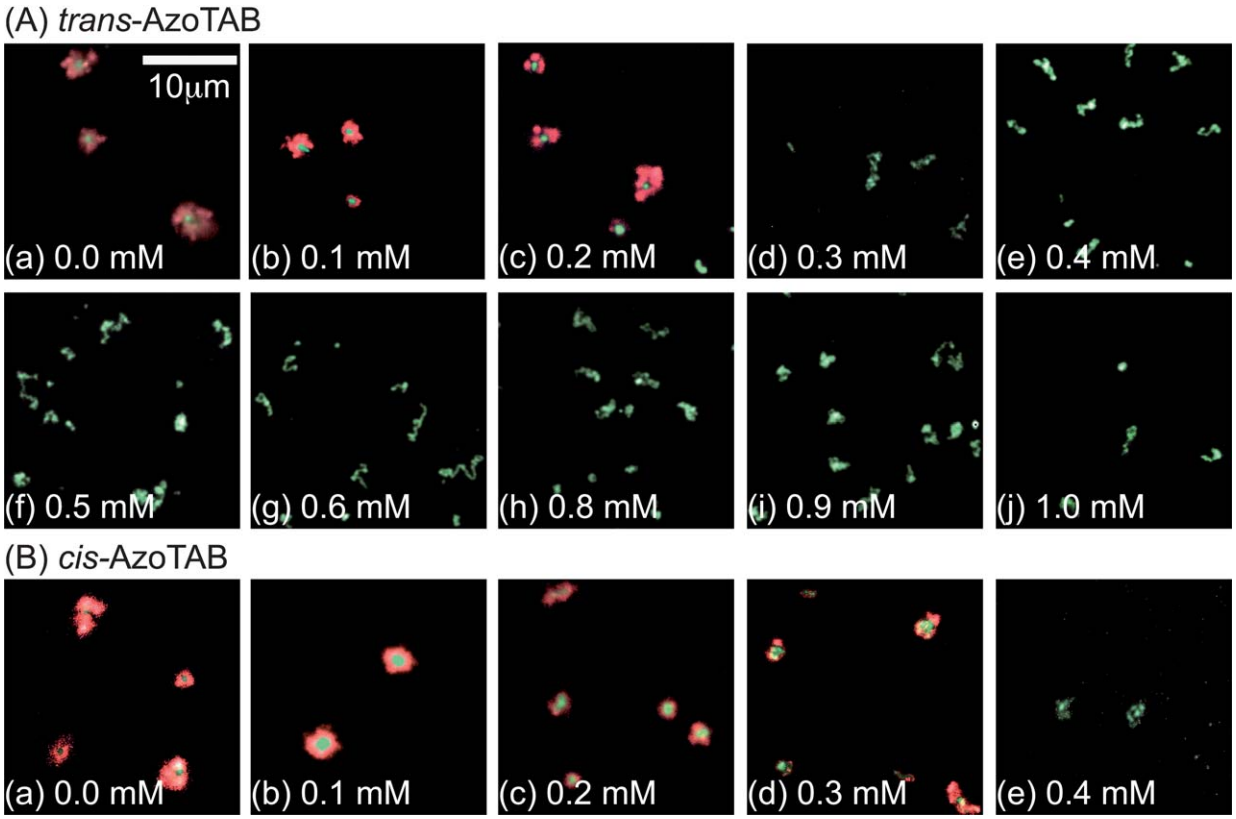

Fig. 3 (A) Effect of the addition of different *trans*-AzoTAB concentrations to end-grafted DNAs in 120 mM tris-borate-EDTA buffer (TBE) solution. Red halos in figures (a)–(c) indicate DNA mobility as explained in Fig. 2. The chain conformations freeze for *trans*-AzoTAB concentrations above 0.3 mM. (B) A similar study with different *cis*-AzoTAB concentrations. With this AzoTAB isomer the chain conformations freeze only above 0.4 mM.

[AzoTAB] $\geq$ 0.3 mM, the disappearance of the red halo indicates that all DNA molecules are in a frozen conformation. Images taken at 2 mM (not shown) also show a frozen configuration. We measured the fraction of the frozen chains for a given AzoTAB concentration by the fraction, computed over several composite images, of the green-only DNAs compared to the total DNA number. The results of the evolution of the frozen fraction with AzoTAB concentration are shown in Fig. 4. The figure also shows in the inset the compaction of T4 DNA chains in the bulk, measured by their maximum extension under an optical microscope as described previously.[8] T4 DNAs are often used for such purposes since they are larger than λ-DNAs and allow for an easier and more precise size determination of the diffusing chains under a fluorescence microscope. Since the compaction in the bulk does not depend on chain size, this provides for a useful comparison with the corresponding behavior of end-grafted λ-DNA. As Fig. 4 shows, the freezing of the end-grafted chains occurs at concentrations below the nominal AzoTAB concentration required for complete chain collapse in the bulk, and the transition from a mobile to a frozen state is sharper than the coil to globule transition in the bulk. This shows that the surfactant binder is able to induce chain-surface interactions at concentrations where the known bulk-like intra-chain interactions start to play an effective role.

In order to further investigate this point, we measured the lateral extension of the end-grafted chains by computing the light-intensity weighted average of the square deviations $(x - x_{CM})^2$ and $(y - y_{CM})^2$ from the center of mass positions x_{CM} and y_{CM} of the light distribution $I(x,y)$, $\langle (x - x_{CM})^2 + (y - y_{CM})^2 \rangle = \sum((x - x_{CM})^2 + (y - y_{CM})^2)/\sum I(x,y)$ with $x_{CM} = \sum x\, I(x,y)/\sum I(x,y)$ and $y_{CM} = \sum y\, I(x,y)/\sum I(x,y)$. The DNAs lateral extension $R = \langle (x - x_{CM})^2 + (y - y_{CM})^2 \rangle^{1/2}$ is displayed in Fig. 5. In the absence of AzoTAB, we obtained a value $R = 0.45\ \mu m \pm 0.06\ \mu m$, of the same order of magnitude of $\sqrt{2}R_g$, the expected two-dimensional projection of the second moment of the monomer concentration distribution for a Gaussian chain of radius of gyration $R_g = (L\ell_p/3)^{1/2} \simeq (16.5 \times 0.05/3)^{1/2} = 0.5\ \mu m$, where we assume a DNA contour length $L \simeq 16.5\ \mu m$ and a persistence length $\ell_p \simeq 0.05\ \mu m$. As the AzoTAB concentration increases, the lateral size increases up to the freezing transition, where it stays roughly constant until it starts to decrease again for concentrations larger than 0.8 mM to reach a constant value above 1 mM.

Most DNA conformations at intermediate concentrations 0.3–0.8 mM can perhaps be better described as resulting from a random lacework. Under the optical microscope, the vertical position where the maximum fluorescence of such conformations can be captured is almost coincident with the surface itself, showing a much reduced vertical extension when compared to the free chains. Experimental evidence suggests then that the chains display an almost two-dimensional random walk, as sketched for the adsorbed chain in Fig. 1. However, a purely two-dimensional self-excluded random walk is not likely to have been achieved in our case. Indeed, by assuming that the polymer has $N = L/\ell_p \simeq 330$ segments, one expects a relative increase of the lateral dimensions $R_{2D}/R \sim N^{3/4-\nu}$,[15] with ν either the excluded

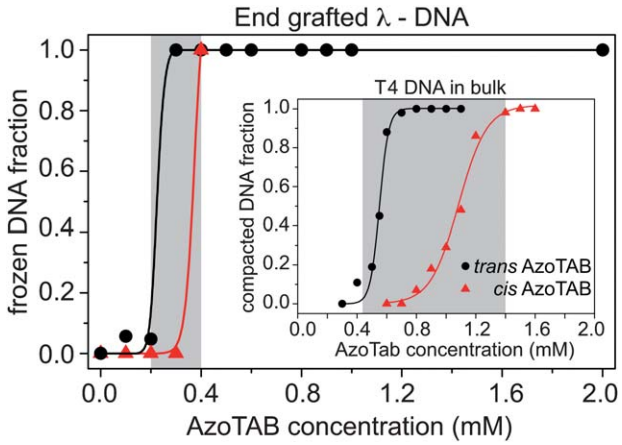

Fig. 4 Fraction of end-grafted lambda-phage DNAs with frozen conformations at different concentrations of (•) *trans* and (Δ) *cis*-AzoTAB, in TBE buffer solution. The immobilized fraction was counted from the number of DNAs without red halos in the composite images described in Fig. 2. While for *trans*-AzoTAB solutions the chain conformations freeze above 0.3 mM, a similar result is only achieved for *cis*-AzoTAB solutions above 0.4 mM. The grey region shows the concentration window where changes in DNA mobility can be expected upon isomerization of the AzoTAB molecule. The inset displays results from a study in bulk of T4 DNA chains in the same buffer solution and different concentrations of (•) *trans* and (△) *cis*-AzoTAB. Compaction of the chains is achieved above 0.6 mM of *trans*-AzoTAB, and above 1.2 mM of its *cis* isomer. The grey area in the inset shows where the compaction state can be modified by a change of the isomeric form of AzoTAB. Note that this grey area in the bulk experiments is wider than the grey area for end-grafted chains. Also the compaction transition in the bulk is less sharp that the freezing transition on the surface.

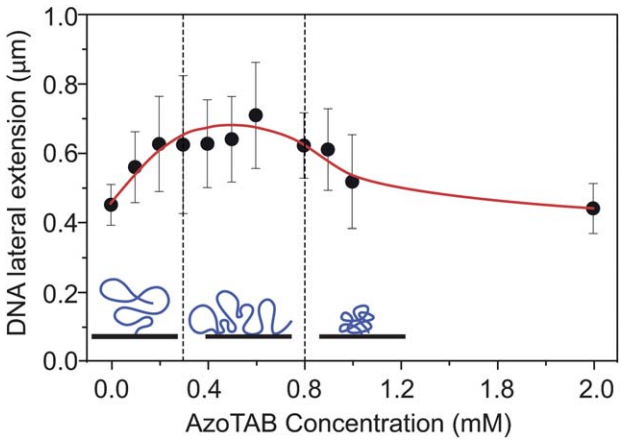

Fig. 5 Lateral extension of lambda-phage DNA's conformations in a TBE buffer with different concentrations of *trans*-azoTAB. Size is here measured by the square root of the mean square displacement in two-dimensions, computed from averages weighted by the light distribution. In the pure TBE buffer, the size of DNAs was 0.45 μm ± 0.06 μm. The first three points for which the average size increases correspond to mobile DNA conformations, while frozen conformations display roughly constant lateral dimensions. For concentrations above 0.8 mM the curve shows that the DNA size is noticeably reduced.

volume exponent $\nu = 0.6$ or, more likely, $\nu = 0.5$ for the case of semi-flexible chains as DNAs, where fully developed swelling statistics require much longer chains.[16,17] Even a conservative estimate leads thus to $R_{2D}/R \sim 2.5$, significantly larger than the 1.5 value obtained in our experiments. Chains confined vertically over a distance D display instead a ratio $R_{2D}/R = (R/D)^{1/4}$. With $R_{2D}/R = 1.5$ we estimate the confinement distance at roughly $D \sim R/5 \sim 0.1$ μm, of the order of the smallest vertical displacement that we can detect with the z-positioning system of our microscope, and thus consistent with the observation that the maximum intensity is vertically coincident with the surface.

Images from chains in a solution with more than 0.8 mM AzoTAB present more compact conformations, also localized at the surface, that can be represented as the globule-like shape in Fig. 1. The transition above 0.8 mM from an extended adsorbed conformation to a compact adsorbed conformation is also compatible with data from bulk DNA—see inset of Fig. 4—showing that intra-chain attractions play a predominant role above such concentration, leading to the collapse of the chains. Note that under our experimental conditions, chains frozen first from solutions with intermediate AzoTAB concentrations 0.3–0.8 mM do not further compact following an increase in the concentration of the solution. This suggests that the compact conformations observed at the large concentrations are formed when intra-chain bonds can form before a strong attachment to the surface precludes further chain rearrangements.

2.2 End-grafted DNAs in a *cis*-AzoTAB solution

We also monitored the conformations of end-grafted λ-phage DNA under the same conditions, except for the added AzoTAB isomer, used here in its *cis* configuration. This more polar form of the cationic surfactant[12] is known to exhibit a smaller affinity to the DNA molecules.[10] In the bulk, for instance, the minimal concentration to achieve full compaction is 0.7 mM and 1.4 mM for *trans* and *cis* isomers, respectively (inset of Fig. 4). In the end-grafted configuration, the composite images of Fig. 3B show that the chains exhibit significant mobility up to 0.4 mM of *cis*-AzoTAB, to be compared to the threshold value of 0.3 mM for the *trans* isomer. Above 0.4 mM the chain behavior and the physical characteristics such as vertical or lateral dimensions are similar to those of the frozen conformations observed in *trans*-AzoTAB solutions. There is thus an AzoTAB concentration window between 0.3 mM and 0.4 mM where one might expect to induce a transition from a frozen to a free state of the DNA coils upon the isomerization of the molecule.

2.3 Effect of light on the adsorbed DNAs

Fig. 6(a) recalls that the conformations of end-grafted λ-DNA freeze due to interactions with the surface, above a concentration of [*trans*-AzoTAB] > 0.3 mM, but require more than 0.4 mM for a solution of *cis*-AzoTAB. For an intermediate concentration, say of 0.35 mM of AzoTAB, one hypothesizes transitions from the frozen, surface-adsorbed conformations to a mobile non-adsorbed state of the end-grafted chain by irradiating the sample with UV-light, thus inducing an isomeric transformation of the surfactant from its *trans* to its *cis* form. That partial or total mobility is recovered can be confirmed by direct observation

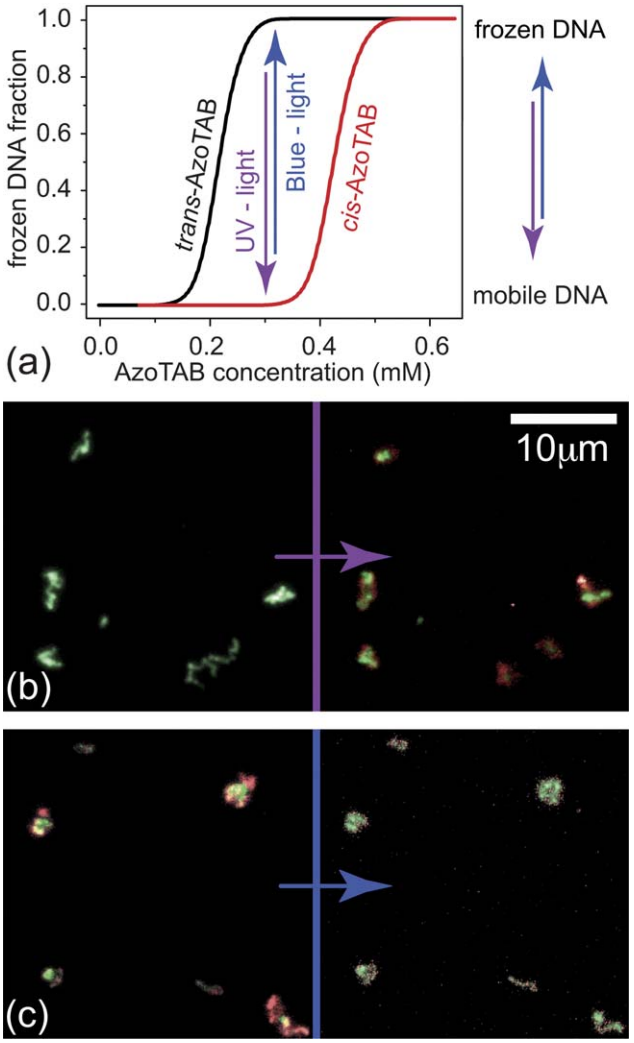

Fig. 6 Light induced changes in the conformations of end-grafted DNAs in 120 mM tris-borate-EDTA buffer (TBE) solution with 0.3 mM AzoTAB. (a) Scheme showing the AzoTAB concentration window where end-grafted lambda-DNAs can be photoswitched between a frozen and a mobile fluctuating state. (b) Initially frozen DNAs in a solution of 0.3 mM *trans*-AzoTAB recover their mobility after being exposed to UV irradiation (330–380 nm). (c) Initially mobile DNAs in a solution of 0.3 mM *cis*-AzoTAB freeze under blue light (450–490 nm).

under a microscope, and also by our mobility analysis displayed in Fig. 6(b). Conversely, illumination of the sample with blue light induces a transformation from the *cis* to the *trans* isomer, bringing initially mobile DNAs in a 0.3 mM *cis* solution into a frozen, adsorbed state as depicted in Fig. 6(c).

Finally, we investigate the kinetics of the light induced transformations. Fig. 7 shows a typical experiment performed by starting with a 0.3 mM *trans*-AzoTAB solution where chains are frozen. Exposure of the sample to UV irradiation under the microscope for 60 s leads to a transformation of the *trans* molecules in the field of view of the microscope into their *cis* isomer. After the UV light is turned off at time $t = 0$, the DNA molecules are observed under blue light. They exhibit a significant mobility during the first few seconds but progressively freeze their conformations. This is due not only to the isomerization under blue light but it is also due to the diffusion of *trans*

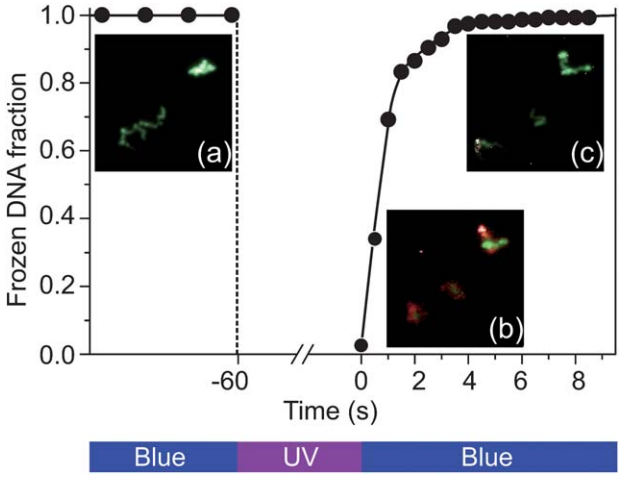

Fig. 7 Kinetics of the transformations between frozen and mobile states of end-grafted λ-phage DNAs in a TBE solution with 0.3 mM AzoTAB. The DNAs are initially frozen in 0.3 mM *trans*-AzoTAB. After being exposed for one minute to UV-illumination under the optical microscope, the DNAs recover their mobility. Diffusion into the observation field of neighboring *trans*-AzoTAB molecules gradually freezes again the DNAs conformations.

molecules from the sample into the field of view. Indeed, molecules of a few nanometres in size have a diffusion coefficient of the order of 10^{-9} m^2s^{-1}, and take thus about 10 s to fully diffuse into a region of 10^{-8} m^2, the typical area of the field of view under our operating conditions.

3 Materials and methods

3.1 AzoTAB synthesis

Azobenzene trimethylammonium bromide (AzoTAB) was synthesized as in Diguet *et al.*,[10] according to a procedure adapted from Hayashita *et al.*[18] Surfactant purity was 99% determined by GC and by 250 MHz H and C NMR spectroscopy.

3.2 Functional DNAs, streptavidin-coated substrates and end-grafted DNA carpets

Double-stranded λ-phage DNA (48502 base pairs, BioLabs) were end-functionalized with two single-stranded oligomers (MWG-Biotech): one end was labeled with biotin, while the other end was labeled with digoxigenin (DIG).[14] After end-labelling, the DNAs were purified through a Nick column (Pharmacia Biotech), diluted in TBE (tris-borate-EDTA buffer, Sigma-Aldrich), and finally stained with YOYO-1 (Invitrogen), an intercalation fluorescent dye, at a 1 : 4 ratio of YOYO per base pair.

The method of preparation of single end-grafted DNA carpets has been described previously by Hisette *et al.*[14] Briefly, cover glasses of 30 mm, from Menzel-Gläser were first cleaned with a piranha solution (75% of H_2SO_4 (97%, Sigma-Aldrich) and 25% of H_2O_2 (30%, Sigma-Aldrich)), and then immediately used after rinsing with milli-Q water. The cleaned glasses were

immersed into an ethanol solution of 2% APTES (3-aminopropyltriethoxysilane, Sigma-Aldrich) for 1 h, then rinsed first with ethanol and then with milli-Q water. The silane layer is stabilized in the oven at 100 °C for one hour and finally kept in dark dry conditions until further use. These silanised glasses were then incubated with glutaraldehyde (8%, Polysciences) for 30 min, rinsed with PBS, and then incubated with a PBS solution of 0.1 mg mL^{-1} streptavidin (Sigma-Aldrich) for one hour. After a final rinsing in TBE, the streptavidinated substrates were kept under humid conditions and used within 2 h.

Streptavidinated substrates were incubated for a few minutes with a 2 μg mL^{-1} biotinylated DNA solution, and gently rinsed with TBE. Special care was taken to avoid any contact between the DNA carpet and air. Due to the strong specific adhesion between biotin and streptavidin, the procedure led to dilute single end-grafted DNA carpets as readily observed by optical fluorescence microscopy.

3.3 Fluorescence microscopy

Fluorescence images were obtained using indifferently inverted microscopes TE200 or TE2000 (Nikon, Japan), equipped with a 100× oil immersion objective. A fluorescence filter block (EX 450–490/DM 505/BA 520 nm) was used for DNA observation, and a second block (EX 330–380/DM 400/BA 420 nm) was used to induce the *trans* to *cis* conformation transition of AzoTAB. Pictures were recorded *via* a digital camera (Hamamatsu EM-CCD, Japan) at a rate of *circa* 10 frames per second, and analyzed using homemade software.

3.4 Observation cell

A homemade observation cell was used to observe the end grafted DNA carpets. The cell enables the slow exchange of the liquid surrounding the carpet directly under the microscope. Briefly, a Teflon® spacer is placed in between two glass slides, one of which being the cover glass supporting the DNA carpet. Two Teflon® tubes (diameter 1.0 mm) are inserted into the spacer. One of the tubes is connected to a syringe while the other is connected to a container. Injection of one millilitre of a liquid into the cell results in a complete exchange of the liquid contained in the cell. Special care has been taken to avoid too strong shear rates during the liquid exchange stage, by ensuring, under the microscope, that the DNA molecules were almost unperturbed by the induced fluid flow.

3.5 Motion detection from image analysis

Our motion analysis is performed on a sequence of several tens of images of a given region of the surface with end-grafted DNA, captured at a typical rate of five images per second, *i.e.* corresponding to roughly ten second sequences. Our observation was performed under attenuated light for the YOYO excitation, thus reducing photo-bleaching, and a high gain level compensating for the relatively low emission power of YOYO, with a good background to signal ratio: this was obtained with an EM-CCD camera (Hamamatsu, Japan). The time dependence of the intensity for each pixel of the image is first stored over the whole time sequence, then, a linear fit of these data is calculated for each pixel, with the corresponding average square difference between the data and the fitting line a quantity known as χ^2. Finally, a new image is built that converts the χ^2 values of each pixel to a grey-level image that can be visualized on the screen, by simply renormalizing the range of measured χ^2 values over the whole image, to the 0–65535 range of a 16 bit image. Such a measurement is shown in Fig. 2A(e) in the red channel of a RGB image. As the figure shows, the pixels of the image in the center of the DNA region appear as dark pixels, corresponding to weak values of χ^2. Here in the center, above the grafting point, the signal is dominated by consistently high values of the average light intensity and therefore by low relative fluctuations around the average. Conversely, the immediate periphery of the central dark region displays a ring-like region of higher χ^2 values. In this region, the intensity fluctuations are comparable to, or larger than, the average intensity. Far from the DNA the image is dark, showing a good signal-to-noise ratio. By superimposing this image with Fig. 2A(d) that represents the fluorescence average intensity image of the same region displayed in the green RGB channel, one obtains the composite Fig. 2A(f). The red halo of the composite image allows easy identification of the fact that the chains exhibited a significant mobility in the image sequence analyzed. When the DNA mobility is reduced either by strong attractive interactions with the surface, or by intra-chain attractions, the red halo vanishes, as displayed in Fig. 2B(e,f). In general, one would expect these halos to be circularly symmetric, which is indeed the case when the measurement is made over a large enough number of images.

4 Conclusions

Exposure of DNA molecules to a solution of nucleic acid binders is known to result in collapse of the chains above a typical threshold concentration, due to intra-chain attractive interactions mediated by the binders. Concentration thresholds are a function of the affinity of the binders, high affinity binders inducing DNA condensation at lower concentrations. The cationic surfactant AzoTAB[8] used in this work is a DNA binder with two photoresponsive isomeric states. Illumination of the molecule with UV-light leads to the *cis* form of the isomer that has lesser affinity than the *trans* isomer. Transition from the *cis* to the *trans* isomers can be obtained for instance by irradiation with blue light. The different binding affinities of the isomers result in two different condensation thresholds, found for instance for T4 DNA in a 120 mM tris-borate-EDTA buffer (TBE) solution at 0.6 mM and 1.2 mM AzoTAB. Within this concentration window, collapse and expansion of the DNAs can be obtained by photo-switching between the two isomeric forms.

In our work, we studied λ-phage DNAs end-grafted to a streptavidinated surface and found attractive interactions between the DNAs and the streptavidin substrate, occurring at lower binder concentrations than the corresponding bulk thresholds, at 0.3 mM and 0.4 mM AzoTAB, respectively, for the *trans* and the *cis* forms. The hierarchy of affinities between the two isomers is thus the same as the corresponding hierarchy in the bulk. We characterized the end-grafted chain fluctuations observed by fluorescence microscopy with a new method that is able to assign a mobility measure to each image pixel, and therefore to color code for a straightforward interpretation of the fluorescence images.

The induced attractions result in a transition that we quantified with our method, from mobile, fluctuating DNA to DNA with frozen conformations. Here binding between the monomers and the surface results in a flattening of the chain and in the absence of fluctuations of the chain segments at the optical level. Strikingly, these chain adsorption transitions are sharper than the corresponding bulk condensation transitions, and the threshold window where photo-switching can be achieved is narrower. In this window, we showed that initially mobile end-grafted chains can be photo-driven into adsorption by blue light, and that initially frozen DNA can be freed by exposure to UV irradiation in the field of view of the microscope. In this last case, return to a frozen state when the UV light is turned off occurs in a few seconds, compatible with fast chain-surface binding, limited only by the diffusion of the binders into intimate contact with the end-grafted chains.

Our work raises not only a number of important questions but also paves the way for further developments of photoresponsive interfacial polymer structures. For instance, our DNA carpets offer new exciting possibilities for performing photocontrolled transcription/expression experiments[11] on individual, substrate born DNAs. The induced attractions with the surface have precluded in our configuration the fundamental study of the influence of end-grafting on the collapsing transition of long DNA chains. Such a study is within a reasonable reach, requiring further protection of the surfaces against chain binding. Our time sensitivity was also restricted to a few images per second, and only diffusion limited phenomena over a few seconds could be studied in detail. Pushing the limits of temporal resolution would certainly bring in crucial new information about the first moments of the chain-surface binding kinetics.

Acknowledgements

This work was supported by the French Ministry for Higher Education through the German-French IRTG on the Physics of Soft Condensed Matter. Inspirational input from T. Schmatko is also acknowledged.

References

1 B. Zhao, J. S. Moore and D. J. Beebe, *Science*, 2001, **291**, 1023–1026.
2 Y. Park, Y. Ito and Y. Imanishi, *Macromolecules*, 1998, **31**, 2606–2610.
3 D. A. LaVan, T. McGuire and R. Langer, *Nat. Biotechnol.*, 2003, **21**, 1184–1191.
4 S. Samanta and J. Locklin, *Langmuir*, 2008, **24**, 9558–65.
5 E. Eisenriegler, *Polymers near surfaces: conformation properties and relation to critical phenomena*, World Scientific, Singapore, 1993.
6 S. Metzger, M. Müller, K. Binder and J. Baschnagel, *J. Chem. Phys.*, 2002, **11**, 985–995.
7 A. L. M. Le Ny and C. T. Lee, *J. Am. Chem. Soc.*, 2006, **128**, 6400–6408.
8 M. Sollogoub, S. Guieu, M. Geoffroy, A. Yamada, A. Estevez-Torres, K. Yoshikawa and D. Baigl, *ChemBioChem*, 2008, **9**, 1201–1206.
9 M. Geoffroy, D. Faure, R. Oda, D. M. Bassani and D. Baigl, *ChemBioChem*, 2008, **9**, 2382–2385.
10 A. Diguet, N. K. Mani, M. Geoffroy, M. Sollogoub and D. Baigl, *Chem.–Eur. J.*, 2010, **16**, 11890–6.
11 A. Estevez-Torres, C. Crozatier, A. Diguet, T. Hara, H. Saito, K. Yoshikawa and D. Baigl, *Proc. Natl. Acad. Sci. U. S. A.*, 2009, **106**, 12219–12223.
12 A. Diguet, R.-M. Guillermic, N. Magome, A. Saint-Jalmes, Y. Chen, K. Yoshikawa and D. Baigl, *Angew. Chem., Int. Ed.*, 2009, **48**, 9281–9284.
13 J. T. Mannion, C. H. Reccius, J. D. Cross and H. G. Craighead, *Biophys. J.*, 2006, **90**, 4538–4545.
14 M. L. Hisette, P. Haddad, T. Gisler, C. M. Marques and A. P. Schroder, *Soft Matter*, 2008, **4**, 828–832.
15 P. G. d. Gennes, *Scaling concepts in polymer physics*, Cornell University Press, Ithaca, N.Y., 1979.
16 D. Schaefer, J. Joanny and P. Pincus, *Macromolecules*, 1980, **13**, 1280–1289.
17 F. Thalmann, V. Billot and C. M. Marques, *Physical Review E*, 2010, submitted.
18 T. Hayashita, T. Kurosawa, T. Miyata, K. Tanaka and M. Igawa, *Colloid Polym. Sci.*, 1994, **272**, 1611–1619.